Bioinspired mechanically stable all-polysaccharide based scaffold for photosynthetic production

Tuuli Virkkala[a], Sergey Kosourov[b], Ville Rissanen[a], Vilja Siitonen[b], Suvi Arola[a], Yagut Allahverdiyeva[b]*, Tekla Tammelin[a]*

[a]VTT Technical Research Centre of Finland Ltd, VTT, PO Box 1000, FI-02044 Espoo, Finland.
[b]Molecular Plant Biology, Department of Life Technologies, University of Turku, FI-20014 Turku, Finland.
*Corresponding authors:
Prof. Yagut Allahverdiyeva, e-mail: allahve@utu.fi, Molecular Plant Biology, Department of Biochemistry, University of Turku, FI-20014, Turku, Finland.
Prof. Tekla Tammelin, e-mail: tekla.tammelin@vtt.fi, VTT Technical Research Centre of Finland LTD, VTT, PO Box 1000, FIN-02044 Espoo, Finland

Electronic supplementary information (ESI)

Experimental section

Oscillatory stress sweep measurements and wet strength determination

Small deformation oscillatory stress sweep measurements were applied to investigate wet strength of the MLG-Ca^{2+}-TCNF hydrogel film scaffolds, which had been submerged in water or growth medium overnight to allow the matrices to swell prior to the measurements. In the stress sweeps, the solid- and liquid-like behaviour of a material are denoted by the storage modulus (G', unit Pa) and loss modulus (G'', unit Pa), respectively, which describe the capability of a material to store energy elastically and dissipate it into heat. The ratio of G'' to G' represents the loss tangent or damping factor (tan δ = G''/G'). G', G'', and tan δ measure the rest properties of a material in the linear viscoelastic (LVE) region (here at 1 Pa, values are shown in Figure S4). MLG-Ca^{2+}-TCNF hydrogel films behaved as viscoelastic solids with yielding behaviour i.e., they were solids at rest but started to deform when the stress was increased. This was seen from the stress curve as G' being approximately an order of magnitude higher than G'' in the LVE region (Figure S1A). When the stress increased, the energy stored in the storage modulus began to disappear into viscous behaviour as the solid interactions weakened. Ultimately, the hydrogel films started to deform non-linearly as energy was lost into viscous behaviour in an accelerating manner, resulting in crack propagation across the sample as the elastic capacity of the material had been reached and the internal bonds started to break. The critical stress denoting the onset of non-linear, irreversible deformation was determined from the stress-strain curve (Figure S1B) as the oscillation stress value at the point where a 15 – 20% decrease of the slope of the curve from the linear region was seen i.e., where a non-linear relationship between stress and strain was observed. Finally, G' and G'' reach a cross-over point where liquid-like character dominates and the materials starts to flow.

Supplementary figures and tables

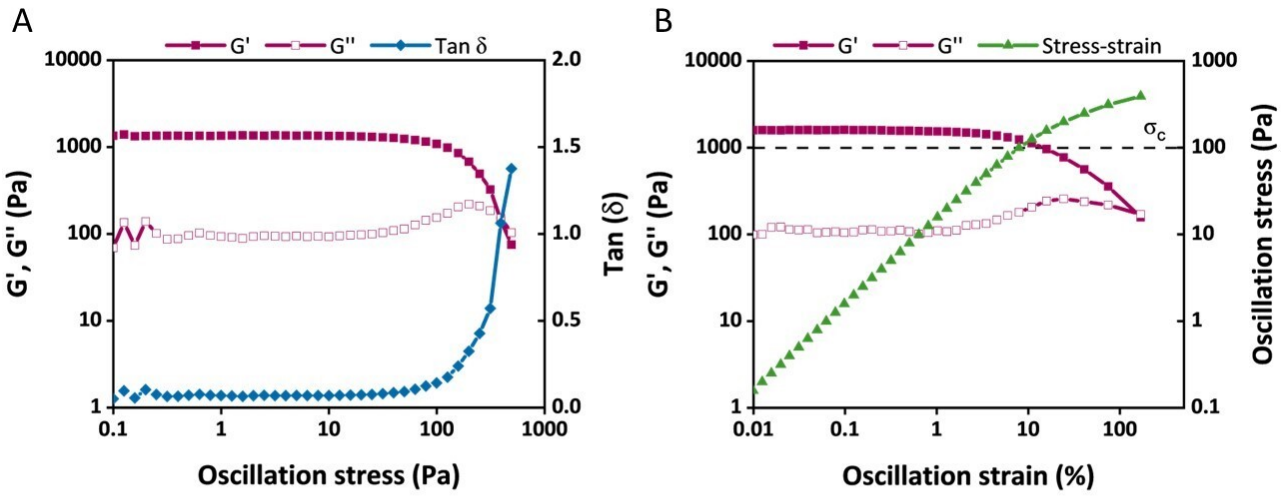

Figure S1. Information gained via small deformation rheology. (A) Typical stress sweep measurement for MLG-Ca2+-TCNF hydrogel films showing G' = storage modulus, G'' = loss modulus, and tan δ = G''/G'. The materials show predominantly elastic behaviour in the LVE region seen by G' being an order of magnitude higher than G''. Sufficiently high stress causes material deformation as seen from G' and G'' starting to decrease and increase, respectively, ultimately reaching a cross-over point where the material starts to flow. (B) The critical stress, i.e. onset of non-linear deformation is obtained from the stress/strain curve from the point where the linear slope decreases 15 – 20%.

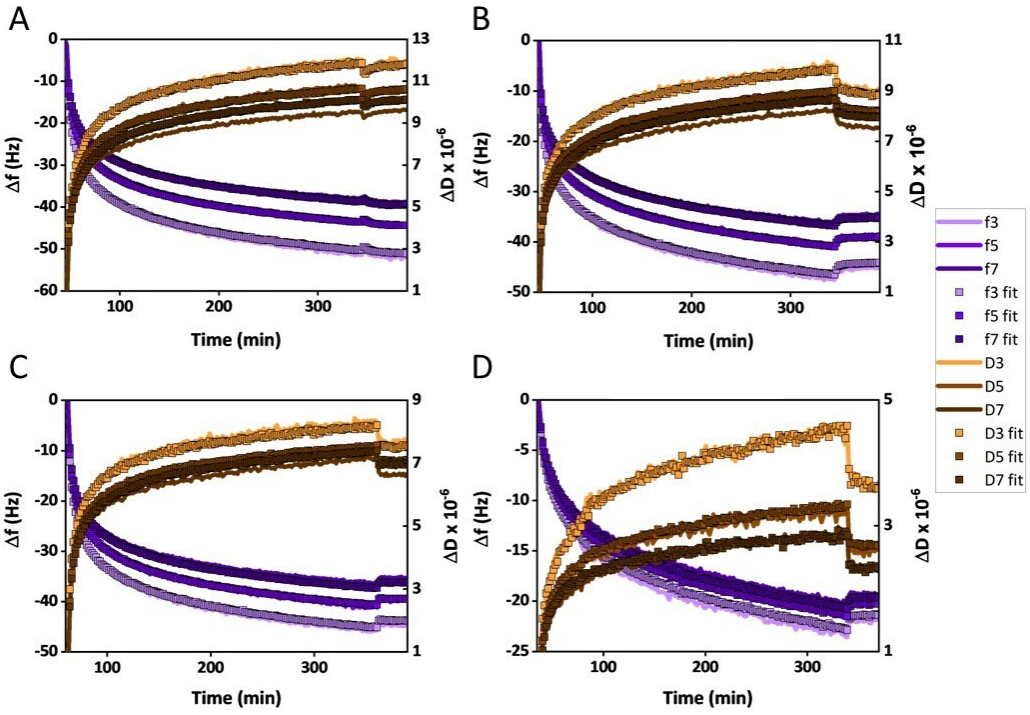

Figure S2. Fitting of Voigt model to MLG adsorption data. Adsorption of 0.01 wt% (A) HVMLG, (B) MVMLG, and (C) LVMLG solutions on TCNF surfaces in water, and (D) LVMLG in BG-11 growth medium. Δf and ΔD as functions of time at 15, 25, and 35 MHz (n = 3, 5, and 7). Lines indicate measured QCM-D data and squares the calculated values with the best fit. Layer density was assumed as 1.05 g cm^{-3}.

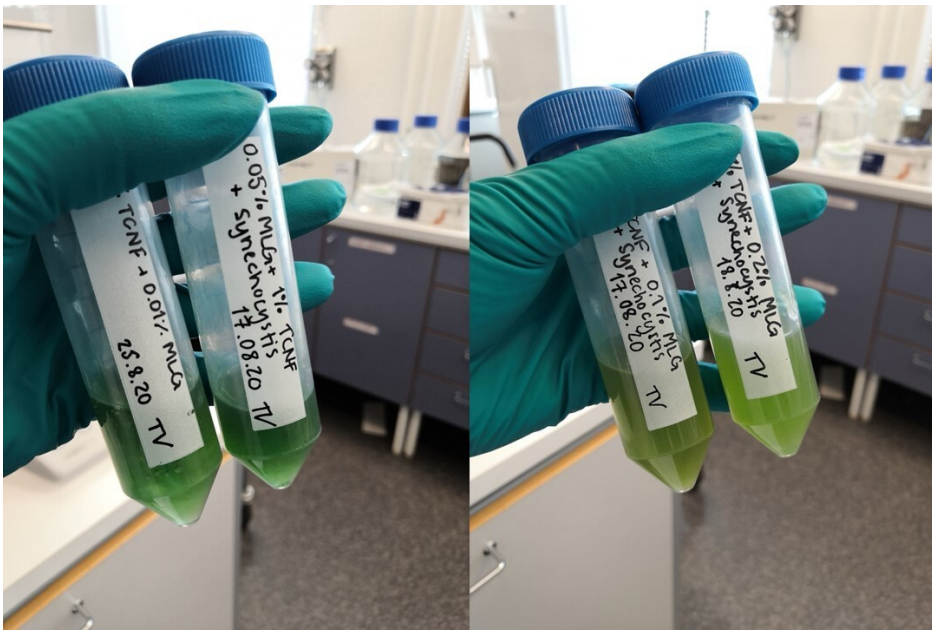

Figure S3. Preliminary visual assessment of matrix biocompatibility. Wild-type Synechocystis cells mixed with 1 wt% TCNF containing HVMLG in 0.01, 0.05, 0.1, and 0.2 wt%. When viable, the cells showcase a bluish green colour. With 0.1 and 0.2 wt% HVMLG, the cells have a slighty more brownish appearance indicative of lower compatibility. 0.05 wt% was therefore used as an upper limit for the amount of HVMLG in the final scaffold.

Table S1. MLG layers at the solid-air interface. Change in frequency and dissipation of dry TCNF and MLG layers in comparison to the TCNF layer at equilibrium, and changes in areal mass as calculated according to Sauerbrey equation (eq 1). Standard deviations are included. 15 MHz, f_0 = 5 MHz, n =3. Assumed layer density is 1.05 g cm^{-3}.

	Δf (Hz)	**ΔD x 10^{-6}**	**Δm (ng cm^{-2})**
TCNF	-46.90 ± 9.9	0.04 ± 0.1	839.35 ± 177.3
HVMLG	-44.68 ± 11.6	0.06 ± 0.1	800.45 ± 213.4
MVMLG	-20.94 ± 5.7	-0.09 ± 0.2	373.85 ± 106.2
LVMLG	-20.11 ± 6.5	0.42 ± 0.5	361.99 ± 117.3
LVMLG (BG-11)	-67.21 ± 6.2	0.03 ± 0.1	1202.06 ± 107.8

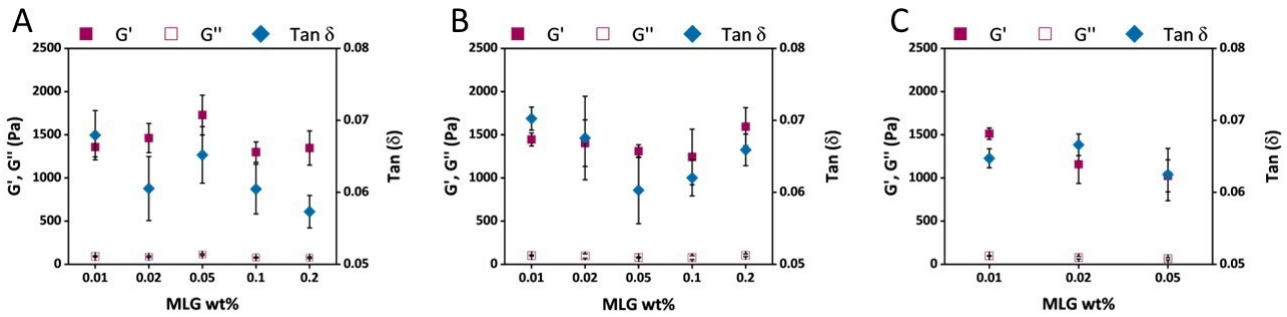

Figure S4. Rest properties of self-standing hydrogel films. G', G'', and tan δ of (A) LVMLG-Ca^{2+}-TCNF, (B) MVMLG-Ca^{2+}-TCNF, and (C) HVMLG-Ca^{2+}-TCNF matrices with varying cross-linker concentration in LVE region at 1 Pa. Standard deviations are shown.

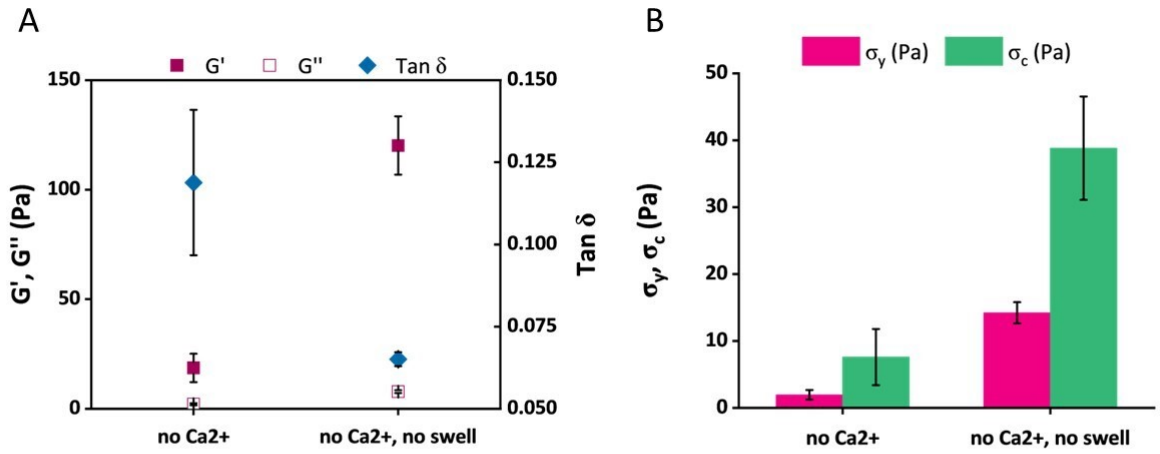

Figure S5. Effect of Ca2+ ions on rheological properties of the hydrogel films. (A) Rest and (B) yield properties of 0.05 wt% LVMLG-TCNF matrices without Ca^{2+}-ions. One set of samples was prepared as the MLG-Ca^{2+}-TCNF matrices in water, and the other in a similar manner without letting the gel films swell overnight prior to the rheological measurements.

Table S2. Effect of cells on rest properties of self-standing hydrogel matrices. Comparison of linear viscoelastic properties of MLG-Ca^{2+}-TCNF matrices prepared in water, BG-11 without cells, and in Synechocystis cell suspension at 1 Pa. HV- and MVMLG-Ca^{2+}-TCNF matrices contain 0.01 wt% cross-linker, and LVMLG-Ca^{2+}-TCNF 0.05 wt% as these amounts seemed to yield the most mechanically stable matrix structures in the submerged conditions. Standard deviations are given.

		G' (Pa)	G'' (Pa)	Tan δ
LVMLG-Ca^{2+}-TCNF	water	1728.25 ± 229.9	111.86 ± 10.0	0.07 ± 4x10^{-3}
	BG-11	1552.90 ± 47.9	102.90 ± 3.3	0.07 ± 2x10^{-3}
	with Synechocystis	1468.19 ± 162.0	96.31 ± 11.1	0.07 ± 3x10^{-3}
MVMLG-Ca^{2+}-TCNF	water	1445.06 ± 75.8	101.47 ± 5.2	0.07 ± 2x10^{-3}
	BG-11	1320.42 ± 50.9	87.36 ± 4.6	0.07 ± 2x10^{-3}
	with Synechocystis	1250.69 ± 201.3	91.34 ± 14.2	0.07 ± 3x10^{-3}
HVMLG-Ca^{2+}-TCNF	water	1511.97 ± 65.7	97.84 ± 4.0	0.07 ± 1x10^{-3}
	BG-11	983.02 ± 68.2	64.11 ± 7.7	0.07 ± 5x10^{-3}
	with Synechocystis	1929.89 ± 214.1	132.89 ± 16.3	0.07 ± 4x10^{-3}

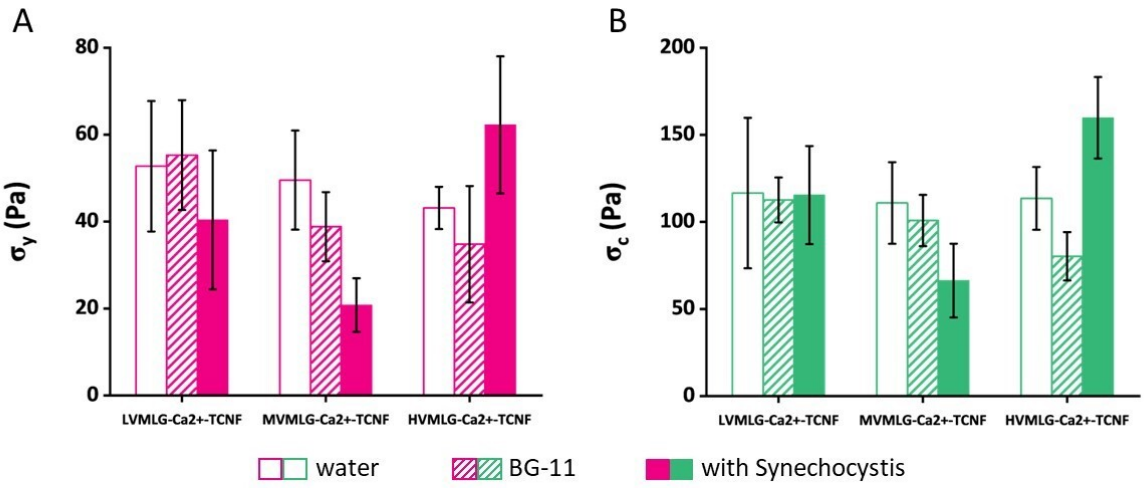

Figure S6. Comparison of yielding behaviour of MLG-Ca^{2+}-TCNF matrices. (A) σ_y and (B) σ_c of the self-standing hydrogel films prepared in water, BG-11 growth medium without cells, and in suspension of Synechocystis cells. Cross-linker concentration of 0.01 wt% was used for HV- and MVMLG-Ca^{2+}-TCNF matrices, and 0.05 wt% for LVMLG-Ca^{2+}-TCNF. Standard deviations are shown.

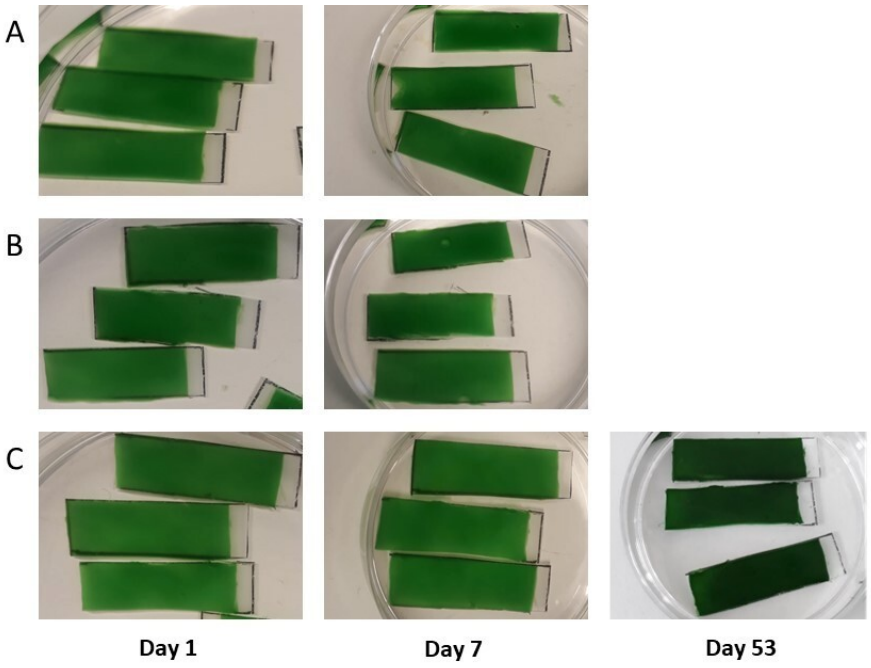

Figure S7. Visual representation of the wild-type Synechocytis cells in MLG-Ca^{2+}-TCNF matrices during the photosynthetic activity monitoring. (A) HVMLG-Ca^{2+}-TCNF, (B) MVMLG-Ca^{2+}-TCNF, and (C) LVMLG-Ca^{2+}-TCNF. Images were taken after 1, 7, and 53 days (LVMLG matrix) of entrapment. All hydrogels remain structurally stable for over 1 week and the LVMLG-Ca^{2+}-TCNF even over 50 days. The bright green color is a visual indicator of the cells remaining viable inside the matrices. Additionally, the darker colour of the LVMLG containing samples at day 53 indicates that the cells have grown inside the matrix, further supporting the notion that the hydrogel is biocompatible.